Electron Transfer in Valence-Trapped Mixed-Valence 2,1′:3,2′:2″,1‴:3″,2‴-Tetrakis(propane-1,3-diyl)-1,1″-biferrocenium Triiodide: Structural, Electrochemical, and Mössbauer Characteristics

Teng-Yuan Dong,* Shu-Hwei Lee, and Ting-Yu Lee

Department of Chemistry, National Sun Yat-Sen University, Kaohsuing, Taiwan, ROC

Received December 18, 1995[⊗]

The X-ray structure determinations of the mixed-valence 2,1′:3,2′:2″,1‴:3″,2‴-tetrakis-(propane-1,3-diyl)-1,1″-biferrocenium triiodide and the corresponding neutral biferrocene and the effects of the interannular trimethylene bridges on the intramolecular electron-transfer rates in both solid and solution states are reported. The X-ray structure of the mixed-valence triiodide salt has been determined at 298 K. The corresponding neutral biferrocene crystallizes in a hexagonal space group. In common with most mixed-valence compounds, the triiodide salt in CH_2Cl_2 have an intervalence transition band at 4904 cm^{-1}. The calculated rate constant of intramolecular electron transfer is 1.21×10^{12} s^{-1}. The Mössbauer results indicate that the mixed-valence triiodide salt has a valence-trapped electronic structure (electron-transfer rate less than $\sim 10^7$ s^{-1} in the solid state). We believe that the most important factor controlling the rate of electron transfer in the solid state in the triiodide salt is the degree of coplanarity between the two Cp rings in the fulvalenide bridge.

Introduction

Recently, an interesting finding was reported that there is a significant influence on the electron-transfer rate in mixed-valence biferrocenium triiodide salts when the two cyclopentadienyl (Cp) rings associated with each ferrocenyl moiety are tilted from a parallel geometry.[1−4] Such a structural modification of the coplanar relation between the two Cp rings around the Fe ion leads to greater metal−ligand interactions as rings tilt. We previously suggested[4] that the difference in electron-transfer rates for the series of alkylbiferrocenium cations (**1**−**3**; Chart 1) is mainly due to the degree of tilting of the Cp rings. Deviations of the Cp rings from the parallel position were found to correlate quite well with the critical temperature of electronic delocalization−localization in mixed-valence biferrocenium cation.

In the case of **4** (Chart 2), there is a significant influence on the electron-transfer rate when the two Cp rings in the ferrocenyl moieties are linked by an interannular trimethylene bridge.[1,2] The Mössbauer results indicate that compound **4** is delocalized on the Mössbauer time scale above 77 K. Only an unusually large single average-valence quadrupole splitting (ΔE_Q = 1.614 mm s^{-1}) is observed at 77 K. Generally, for a Mössbauer delocalized mixed-valence biferrocenium cation, the value of ΔE_Q is expected to be $\sim$1.2 mm s^{-1}. The unusual large quadruple splitting of **4** indicates that there is a strong metal−ligand interaction caused by the interannular trimethylene bridge. We also prepared

Chart 1

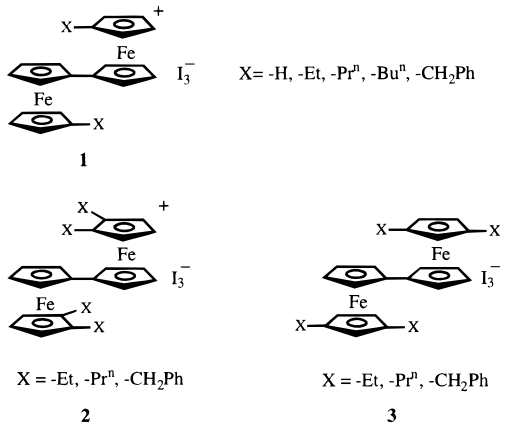

a series of model compounds **5**−**13** to explain this unusual observation and to understand the influence of the interannular bridge on the electronic ground state.[5−7] As we expected, a large quadruple splitting for the ferrocenium moiety was observed in the Mössbauer spectra of **5**−**13**. The Mössbauer studies clearly indicate that the electronic ground state of the Fe(III) metallocene in **5**−**13** is not the pure $^2E_{2g}$ state. Bending back the Cp rings leads to an increase of $d_{x^2-y^2}$, d_{xy}-ring overlap. The metal nonbonding orbitals start to interact with the ligand π orbitals. Under these conditions the iron ions lose some degree of their Fe(III) character, and this results in an increase in ΔE_Q because each iron ion is closer to Fe(II) in its properties. We now show that the physical properties of the new constitutional isomer **14** considerably expand our understanding of the effects of ring tilting on biferrocenium electronic structure.

[⊗] Abstract published in *Advance ACS Abstracts,* April 1, 1996.

(1) Dong, T.-Y.; Chou, C. Y. *J. Chem. Soc., Chem. Commun.* **1990**, 1332.
(2) Dong, T.-Y.; Lee, T. Y.; Lin, H. M. *J. Organomet. Chem.* **1992**, 427.
(3) Dong, T.-Y.; Chang, C. K.; Huang, C. H.; Wen, Y. S.; Lee, S. L.; Chen, J. A.; Yeh, W. Y.; Yeh, A. *J. Chem. Soc., Chem. Commun.* **1992**, 526.
(4) Dong, T.-Y.; Huang, C. H.; Chang, C. K.; Wen, Y. S.; Lee, S. L.; Chen, J. A.; Yeh, W. Y.; Yeh, A. *J. Am. Chem. Soc.* **1993**, *115*, 6357.
(5) Dong, T.-Y.; Lin, S. H. *J. Organomet. Chem.* **1992**, *426*, 369.
(6) Dong, T.-Y.; Lee, T. Y.; Lee, S. H.; Lee, G. H.; Peng, S. M. *Organometallics* **1994**, *13*, 2337.
(7) Dong, T.-Y.; Lee, S. H. *J. Organomet. Chem.* **1995**, *487*, 77.

S0276-7333(95)00968-X CCC: $12.00

Chart 2

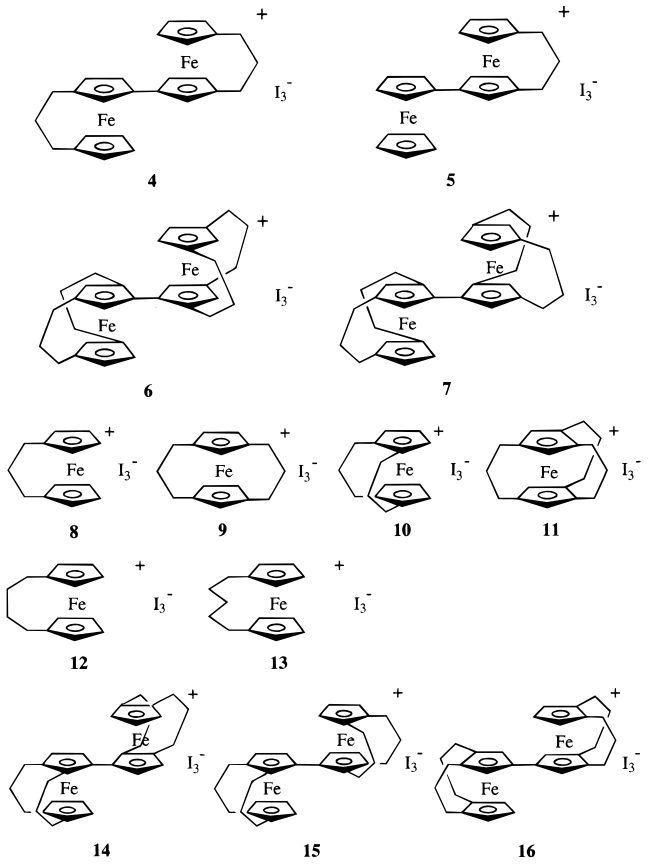

Scheme 1

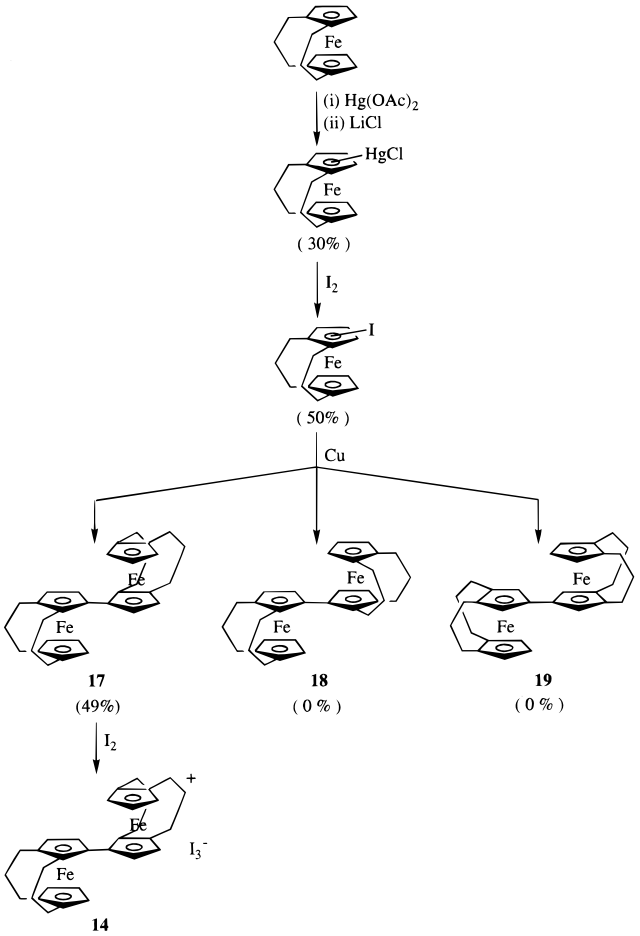

Results and Discussion

Compound **14** was prepared by coupling iodo-1,1′:2,2′-bis(propane-1,3-diyl)ferrocene using activated Cu as a catalyst (Scheme 1). In comparison with the coupling reaction of iodo-1,1′:3,3′-bis(propane-1,3-diyl)ferrocene, we could not isolate the two constitutional isomers **18** and **19**. In the case of the coupling reaction of iodo-1,1′;3,3′-bis(propane-1,3-diyl)ferrocene, the two constitutional isomers **6** and **7** were isolated.[6] This difference in product possibly originates in the electronic control of the steps of mercuration and iodination and the steric control of the step of Ullman coupling.

X-ray crystallographic studies of **14** and **17** were undertaken to elucidate the structures, which are difficult to determine with certainty solely with NMR spectroscopy. It also help us to understand the geometric influences on the rate of electron transfer in mixed-valence biferrocenium cation. Before the new physical date are described, a summary of single-crystal X-ray structural results obtained for **14** and **17** will be presented.

Structural Studies. The results of our crystallographic study at room temperature show that **14** and **17** crystallize in the hexagonal space group $P6_122$ and the orthorhombic space group *Pccn*, respectively, and their molecular structures are shown in Figures 1 and 2. Selected bond distances and angles are given in Table 1. They do not exist in a trans conformation with the two iron ions on opposite sides of the planar fulvalenide ligand observed for most biferrocenium cations.[8,9] Only a few cis conformation biferrocenes are known,[10] and in all case, the molecule is held in a cis conformation by a bridge between the 2,2′ positions of the fulvalenide ligand. As can be seen in Figures 1 and 2, the two metallocene units in **14** and **17** are twisted relative to each other. The two Cp rings in the fulvalenide bridge are not coplanar, and the dihedral angles between the Cp rings of the fulvalenide ligand in **14** and **17** are 78.2 and 64.0(4)°, respectively. We believe that the degree of coplanarity between the two Cp rings in the fulvalenide bridge plays an important role in determining the magnitude of the electron-transfer rate. A detailed discussion will be presented in the section on Mössbauer characteristics.

In **14**, the average distance from the iron atom to the two Cp rings is 1.65(1) Å, which is less than the value of 1.70 Å found for ferroceniums.[11] The mean bond distance from the Fe atom to the ring carbon atoms in **14** is 2.05(2) Å, which is less than the value of 2.075 Å found for ferroceniums.[11] In the neutral compound **17**, the mean bond distance from the Fe atom to the ring carbon atoms is 2.03(1) Å, which is also less than the value of 2.045 Å found for ferrocenes.[12] Possibly, this is due to the compression of the interannular trimethylene bridge on the Fe atom. Furthermore, the average Fe−Cp and Fe−C distances in **14** are marginally larger

(8) Dong, T.-Y.; Hendrickson, D. N.; Iwai, K.; Cohn, M. J.; Rheingold, A. L.; Sano, H.; Motoyama, S. *J. Am. Chem. Soc.* **1985**, *107*, 7996.

(9) Konno, M.; Hyodo, S.; Iijima, S. *Bull. Chem. Soc. Jpn.* **1982,** *55*, 2327.

(10) Zhang, W.; Wilson, S. R.; Hendrickson, D. N. *Inorg. Chem.* **1989**, *28*, 4160 and references therein.

(11) Mammano, N. J.; Zalkin, A.; Landers, A.; Rheingold, A. L. *Inorg. Chem.* **1977**, *16*, 297.

(12) Seiler, P.; Dunitz, J. D. *Acta Crystallogr., Sect. B* **1979**, *35*, 1068.

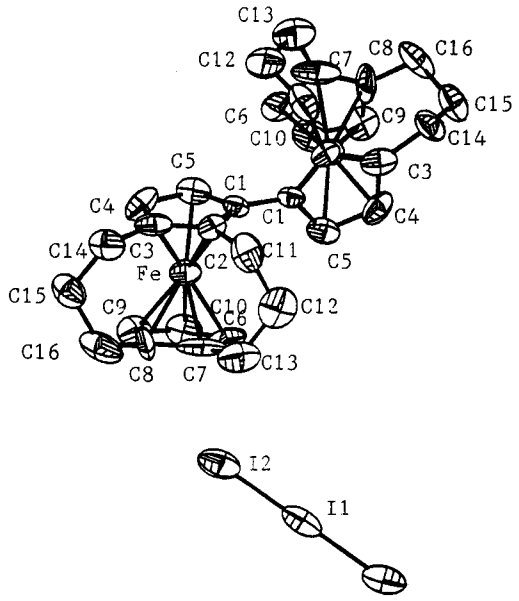

Figure 1. ORTEP drawing of mixed-valence **14**.

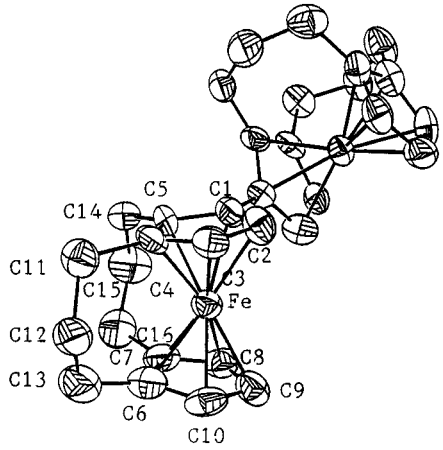

Figure 2. ORTEP drawing of neutral compound **17**.

than that in the corresponding neutral biferrocene **17**. Such an increase in Fe−Cp and Fe−C distances has been observed when ferrocene is oxidized to the corresponding ferrocenium cation.[11,13]

The respective dihedral angles between the two least-square planes of the Cp rings for a given ferrocenyl moiety in **14** and **17** are 16(1) and 13.3(6)°, while the two Cp rings in each ferrocenyl moiety are nearly eclipsed with average staggering angles of 2(1) and 1.6(1)°. The triiodide anion in **14** shows a symmetric structure. The I−I bond distance is 2.924(2) Å, which is in accord with the accepted value of 2.92 Å reported for the free triiodide ion.[14] The angle $I_2-I_1-I_2$ is 176.9(1)°.

Electrochemical Results. As shown in Figure 3, the neutral compound **17** undergoes two successive reversible one-electron oxidations to yield the mono- ($E_{1/2} = 0.205$ V) and then the dication ($E_{1/2} = 0.460$ V). Electrochemical reversibility was demonstrated by the peak-to-peak separation between the resolved reduction and oxidation wave maxima (~75 mV). It has been reported that the magnitude of the peak-to-peak separation ($\Delta E_{1/2}$) gives an indication of the interaction between the two Fe sites.[15] The Fe−Fe interaction increases as the value of $\Delta E_{1/2}$ increases. A comparison of the magnitude of $\Delta E_{1/2}$ of **17** (0.255 V) and **16** (0.326 V) indicates that the magnitude of interaction between the two Fe sites in **17** is rather small. As reported before, there are two possible mechanisms of interaction between the two ferrocenyl moieties: interaction propagated through the fulvalenide bridge and through space. Therefore, the conformational relationship between the

Table 1. Selected Bond Distances (Å) and Bond Angles (deg)

	17	**14**
I1−I2		2.924(2)
Fe−C1	2.052(9)	2.07(2)
Fe−C2	2.06(1)	1.99(2)
Fe−C3	2.04(1)	2.02(2)
Fe−C4	1.99(1)	2.0092)
Fe−C5	2.03(1)	2.07(2)
Fe−C6	2.02(1)	2.07(2)
Fe−C7	2.02(1)	2.00(2)
Fe−C8	2.03(1)	2.06(2)
Fe−C9	2.06(1)	2.10(2)
Fe−C10	2.04(1)	2.10(2)
C1−C1[a]	1.50(2)	1.44(3)
C1−C2	1.41(2)	1.42(3)
C1−C5	1.45(1)	1.38(3)
C2−C3	1.42(1)	1.40(3)
C3−C4	1.43(2)	1.38(3)
C4−C5	1.43(2)	1.48(3)
C6−C7	1.47(2)	1.51(4)
C6−C10	1.43(2)	1.41(4)
C7−C8	1.39(2)	1.38(4)
C8−C9	1.42(2)	1.42(4)
C9−C10	1.40(2)	1.43(4)
I2−I1−I2[b]		176.9(1)
C2−C1−C5	109.0(8)	106(2)
C1−C2−C3	108.9(9)	112(2)
C2−C3−C4	106.9(9)	106(2)
C3−C4−C5	109.6(9)	109(2)
C1−C5−C4	105.7(9)	107(2)
C7−C6−C10	105.4(1)	104(2)
C6−C7−C8	107.0(1)	109(3)
C7−C8−C9	111(1)	109(2)
C8−C9−C10	106(1)	107(2)
C6−C10−C9	111(1)	111(2)

[a] **17**, x, $1 + x - y$, $0.167 - z$; **14**, $1.5 - x$, $0.5 - y$, z. [b] **14**, $0.5 - x$, $0.5 - y$, z.

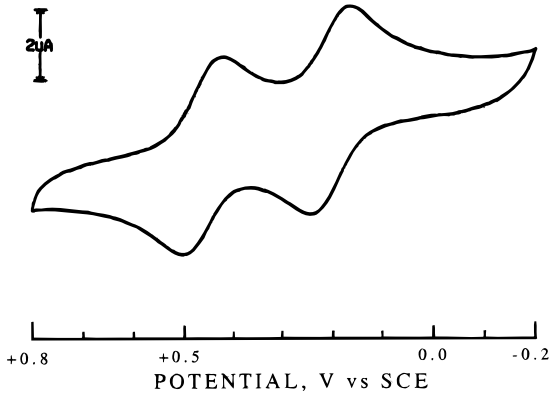

Figure 3. Cyclic voltammogram of **17**.

(13) Dong, T.-Y.; Schei, C. C.; Hwang, M. Y.; Lee, T. Y.; Yeh, S. K.; Wen, Y. S. *Organometallics* **1992**, *11*, 573.

(14) Runsink, J.; Swen-Walstra, S.; Migchelsen, T. *Acta Crystallogr., Sect. B* **1972**, *28*, 1331.

(15) (a) Morrison, W. H., Jr.; Krogsrud, S.; Hendrickson, D. N. *Inorg. Chem.* **1973**, *12*, 1998. (b) Bunel, E. E.; Campos, P.; Ruz, J.; Valle, L.; Chadwick, I.; Ana, M. S.; Gonzalez, G.; Manriquez, J. M. *Organometallics* **1988**, *7*, 474. (c) Atzkern, H.; Huber, B.; Köhler, F,.H.; Müller, G.; Müller, R. *Organometallics* **1991**, *10*, 238. (d) Chukwu, R.; Hunter, A. D.; Santarsiero, B. D.; Bott, S. G.; Atwood, J. L.; Chassaignac, J. *Organometallics* **1992**, *11*, 589.

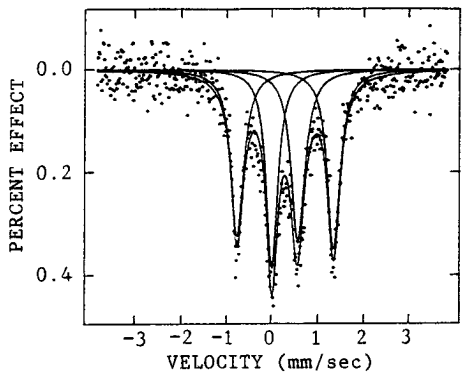

Figure 4. ^{57}Fe Mössbauer spectrum of **14**.

Table 2. ^{57}Fe Mössbauer Least-Squares-Fitting Parameters at 300 K

compd	ΔE_Q (mm/s)[a]	δ (mm/s)[b]	Γ (mm/s)[c]
6	1.766	0.370	0.357, 0.379
	1.079	0.382	0.438, 0.438
7	1.864	0.356	0.259, 0.284
	1.273	0.368	0.285, 0.302
14	2.103	0.397	0.335, 0.361
	0.546	0.402	0.352, 0.303

[a] Quadrupole splitting. [b] Isomer shift. [c] Full width at half-height taken from the least-squares-fitting program. The width for the line at more positive velocity is listed for the doublet. [d] From ref. 6.

two Cp rings of the fulvalenide bridge in ferrocene is dramatically important in determining the magnitude of Fe−Fe interaction. In contrast to most biferrocenes, the two Cp rings of the fulvalenide bridge in **17** and neutral compounds of **15** and **16** are not crystallographically coplanar in the solid-state structure. In the solution state, we found[6] that the two Cp rings of the fulvalenide bridge in neutral compounds of **15** and **16** have to be coplanar in order to have a large Fe−Fe interaction. This is different from the solution-state structure of **17** in which the two Cp rings of fulvalenide bridge are not coplanar. Therefore, compound **17** has a smallest value of $\Delta E_{1/2}$.

In eq 1, the abbreviations [3,3], [2,3], and [2,2] denote the dioxidized salt, the

$$[2,2] + [3,3] \overset{K}{\rightleftharpoons} 2[2,3] \qquad (1)$$

monooxidized salt, and the neutral compound, respectively. From the value of $\Delta E_{1/2}$, the comproportionation equilibrium constant K (2.10×10^4) can be calculated. In the studies of intervalence transition band in the near-IR region, quantitative calculations based on the concentration of [2,3] have been corrected for this equilibrium.

^{57}Fe Mössbauer Characteristics. The various absorption peaks in the ^{57}Fe Mössbauer spectrum (Figure 4) of **14** were fitted to Lorentzian lines, and the resulting fitting parameters are summarized in Table 2. The pattern of this spectrum is two doublets, one with $\Delta E_Q = 0.56$ mm s^{-1} (Fe(III) site) and the other with $\Delta E_Q = 2.11$ mm s^{-1} (Fe(II) site). Furthermore, both doublets have the same area, as deduced by the least-squares fitting. This pattern is expected for a mixed-valence biferrocenium cation which is valence-trapped on the time scale of the Mössbauer technique (electron-transfer rate less than $\sim 10^7$ s^{-1}).[8] We believe that the localized electronic structure of **14** is mainly due to the noncoplanarity of the two Cp rings in the fulvalenide bridge in **14**. The single-crystal X-ray determination of **14** indicates that the π interaction between the two ferrocenyl moieties is destroyed as the linked bond of the two ferrocenyl units is twisted.

Finally, it is necessary to discuss why the ferrocenium moiety in **14** has a smaller value of ΔE_Q in comparison with **5** (0.771 mm s^{-1}),[1,2] **6** (1.079 mm s^{-1}),[6] and **7** (1.273 mm s^{-1}).[6] In general, ferrocenyl groups (electronic ground state $^1A_{1g}$) give spectra characterized by large quadruple splitting in the range of 2.0−2.2 mm s^{-1}, while the spectra of ferrocenium cations (electronic ground state $^2E_{2g}$) are characterized by small or vanishing quadruple splitting.[16] In the case of a Mössbauer-localized mixed-valence biferrocenium cation, the value of ΔE_Q in the ferrocenyl moiety is slightly smaller than what is expected for a Fe(II) ferrocenyl unit and the Fe(III) ferrocenium moiety has a slightly larger ΔE_Q value. This result is a reflection of the mixing of the Fe(II) and Fe(III) moiety into the ground state.[8,16] As mentioned in the Introduction, the unusually large ΔE_Q values of **5**−**7** were explained in terms of an increase of metal−ligand interaction.[6] We suggested that the larger ΔE_Q value is mainly a result of the metal nonbonding orbitals ($d_{x^2-y^2}$, d_{xy}) starting to interact with the ligand π orbitals as the Cp rings are bent back. We also prepared a series of model compounds **5**−**13** to explain the influence of tilt angle on the ^{57}Fe Mössbauer quadruple splitting.[5,7] The tilt angles of the two Cp rings associated with each ferrocenyl moiety for **6**, **7**, and **14** are 14.4(2), 12.9(5), and 16(1)°, respectively. Thus, the magnitude of ΔE_Q value decreases as the tilt angle increases. Of course, this is not consistent with our previous suggestion. Previously, we suggested that the magnitude of the ΔE_Q value increases as the tilt angle increases. Here, we make a reasonable modification. It is possible that the metal−ligand interaction approaches a maximum and then becomes small as the tilt angle continously increases. In our previous paper, we prepared[7] a series of model compounds **8**−**11** to study the relationship between the tilt angle and the magnitude of the ΔE_Q value. We found that the value approaches a maximum ($\Delta E_Q = 0.936$ mm s^{-1}) at the tilt angle of 9.2°. This is what we observe for compound **14** in the ^{57}Fe Mössbauer studies.

Electron Transfer in the Solution State. In common with most mixed-valence compounds, the mixed-valence compound **14** in CH_2Cl_2 has an intervalence transition (IT) band at 4904 cm^{-1}, which is not present for the neutral compound or dioxidized ion. A description of the width of the IT band, the extent of electron delocalization, and the electron-transfer properties of mixed-valence dimers has been given by Hush.[17] Hush has derived an expression for the bandwidth (in cm^{-1}) at half-maximum of the IT band of a localized homonuclear mixed-valence dimer at 300 K as

$$\Delta\nu_{1/2(\text{calcd})} = (2310\nu_{\max})^{1/2} \qquad (2)$$

where $\nu_{\max}$ is the frequency in cm^{-1} of the absorption maximum and the constant is in the unit of cm^{-1}. For a system with harmonic nuclear motion, the energy of

(16) Morrison, W. H., Jr.; Hendrickson, D. N. *Inorg. Chem.* **1975**, *14*, 2331.
(17) Hush, N. S. *Prog. Inorg. Chem.* **1967**, *8*, 391.

Table 3. Absorption Maxima of IT Band and Activation Parameters

		$\Delta\nu_{1/2}$[a]					
compd	ν_{max}[a]	obsd	calcd	ϵ_{max}[b]	α^2	H_{ab}[a]	$10^{-12}K_{et}$
6[c]	4808	2930	2150	3333	0.0214	703	3.26
7[c]	5050	2690	2170	3415	0.0188	692	2.31
14[d]	4904	821	3179	3366	0.0087	457	1.21

[a] In cm^{-1}. [b] Extinction coefficient in M^{-1} cm^{-1}. [c] From ref 6. [d] This work.

activation ΔE^* is related to the energy of the IT band maximum (ν_{max}) by the expression

$$\Delta E^* = {}^1/_4\nu_{max} \quad (3)$$

Furthermore, the magnitude of the delocalization can be obtained by a calculation of the delocalization parameter α^2 and electronic coupling H_{ab} from eqs 4 and 5. In eqs 4 and 5, ϵ_{max} is the extinction coefficient, the

$$\alpha^2 = [(4.24 \times 10^{-4})\epsilon_{max}(\Delta\nu_{1/2})]/(\nu_{max}d^2) \quad (4)$$

$$H_{ab} = \nu_{max}\alpha \quad (5)$$

constant (4.24×10^{-4}) is in the unit of M cm^{-1}, and d is the donor−acceptor distance. The average value (5.1 Å) of the Fe−Fe distances in the series of dialkyl mixed-valence biferrocenium cations is used as the donor−acceptor distance.[8] The rate constant (K_{et}) can be estimated from eq 6, where ν_{et} is the hopping frequency. The absorption maximum and activation parameters calculated from eqs 2−6 were collected in Table 3, together with those for other relevant compounds.

$$K_{et} = \nu_{et}\exp(-\nu_{max}/4K_BT) \quad (6)$$

$$\nu_{et} = (2\pi/\hbar)H_{ab}{}^2(\pi/K_BT\nu_{max})^{1/2}$$

The experimental α^2 value is the average of α^2 values for the ground and excited states. If delocalization is small, the electronic wave functions used for overlap are relatively unperturbed. Thus, α^2 is a direct measure of delocalization in the ground state. As shown in Table 3, there is good evidence for localized valences in **14**.

As illustrated in Table 3, the electron-transfer rate in **14** is slower than those in **6** and **7**. This difference in electron-transfer rate indicates that the interannular trimethylene bridges play an important role in controlling the rate of electron transfer. As discussed in electrochemical studies, the conformational relationship between the two Cp rings in the fulvalenide is critical to the magnitude of Fe−Fe interaction (H_{ab}) in **6**, **7**, and **14**.

Experimental Section

General Information. All manipulations involving air-sensitive materials were carried out by using standard Schlenk techniques under an atmosphere of N_2. Chromatography was performed on neutral alumina (Merck, activity II). The sample of 1,1′:2,2′-bis(propane-1,3-diyl)ferrocene was prepared according to the literature procedure[18] and identified by its melting point, NMR, and mass spectrum.

Mercuration of 1,1′:2,2′-Bis(propane-1,3-diyl)ferrocene. A CH_3OH (120 mL) solution of mercuric acetate (1.3 g, 4.08 mmol) was added dropwise to a hot solution of 1,1′:2,2′-bis-(propane-1,3-diyl)ferrocene (1.8 g, 6.76 mmol) dissolved in 120 mL of absolute CH_3OH and 60 mL of dry benzene. The mixture was refluxed for 18 h, and then LiCl (0.31 g) in 65 mL of hot CH_3OH was added dropwise. A yellow precipitate was formed immediately out of an orange solution. The solvent was removed under vacuum. The resulting yellow powder was put into a Soxhlet extractor and extracted with hexane to yield starting material. Further extraction with CH_2Cl_2 yielded 0.68 g (30%) yellow solid. The crude product was used without further purification.

Iodination of Mercurated 1,1′:2,2′-Bis(propane-1,3-diyl)ferrocene. *N*-Iodosuccinimide (NIS, 1.01 g, 4.53 mmol) in 75 mL of CH_2Cl_2 was added dropwise at 0 °C to 1.41 g (2.81 mmol) of mercurated 1,1′:2,2′-bis(propane-1,3-diyl)ferrocene. The reaction was allowed to warm to room temperature and was stirred overnight. To this solution was added 50 mL of 10% aqueous $Na_2S_2O_3$ followed by 50 mL of 10% aqueous $NaHCO_3$. The organic layer was separated, and the aqueous portion was extracted with 3 × 50 mL portions of CH_2Cl_2. The combined organic layer was washed twice 100 mL of 10% aqueous $NaHCO_3$ and twice with 100 mL of H_2O and dried over $MgSO_4$. The solvent was removed under reduced pressure. The red residue oily was chromatographed, eluting with hexane. The first band was the desired compound (~0.5 g, 50%). The properties of iodo-1,1′:2,2′-bis(propane-1,3-diyl)-ferrocene are as follows. ^{1}H NMR ($CDCl_3$, ppm): 3.8, 4.0 (5H, m, ring protons), 1.5, 2.1 (12H, m, methylene protons). Mass spectrum: M^+ at m/z 392.

Neutral Compound 17. Compound **17** was prepared by the Ullman coupling procedure as shown in Scheme 1. A mixture of iodo-1,1′:2,2′-bis(propane-1,3-diyl)ferrocene (0.6 g) and activated copper (2.4 g) was heated under N_2 at 110−120 °C for 24 h. After being cooled to room temperature, the reaction mixture was repeatedly extracted with CH_2Cl_2 until the CH_2Cl_2 extracts appeared colorless. The extracts were evaporated and chromatographed on neutral Al_2O_3. The first band eluted with hexane yielded the starting material. Continued elution with hexane afforded the desired compound **17** (0.2 g). Compound **17** was recrystallized from benzene/hexane. ^{1}H NMR of **17** ($CDCl_3$, ppm): 4.24 (m, 4H, Cp), 3.77 (bs, 2H, Cp), 3.72 (d, 2H, Cp), 3.48 (bs, 2H, Cp), 1.8−2.3 (m, 16H, $-CH_2-$), 1.4−1.7 (m, 8H, $-CH_2-$). Mp: 108 °C (dec). Mass spectrum: M^+ at m/z 530.

Mixed-Valence Compound 14. A crystalline sample of **14** was prepared by adding a benzene/hexane (1:1) solution containing a stoichiometric amount of iodine to a benzene/hexane (1:1) solution of the corresponding biferrocene at 0 °C. The resulting dark green crystals were filtered out and washed repeatedly with cold hexane. Anal. Calcd for **14** ($C_{32}H_{34}Fe_2I_3$): C, 42.19; H, 3.76. Found: C, 41.38; H, 3.68.

Physical Methods. ^{57}Fe Mössbauer measurements were made on a constant-velocity instrument which has been previously described.[13] Computer fittings of the ^{57}Fe Mössbauer data to Lorentzian lines were carried out with a modified version of a previously reported program.[19] Velocity calibration was made using a 99.99% pure 10 mm iron foil. Typical line widths for all three pairs of iron lines fell in the range 0.24−0.27 mm s^{-1}. Isomer shifts are reported relative to iron foil at 300 K. It should be noted that the isomer shifts illustrated in the figures are plotted as experimentally obtained. Tabulated data are provided.

^{1}H NMR spectra were recorded on a Bruker AMX200 spectrometer. Mass spectra were obtained with a VG250-70S system. The near-IR spectra were recorded from 2300 to 900 nm in CH_2Cl_2 by using 1.0-cm quartz cells with a Perkin-Elmer Lambda 9 spectrophotometer.

Electrochemical measurements were carried out with a BAS 100W system. Cyclic voltammetry was performed with a stationary glassy carbon working electrode, which was cleaned

(18) Hillman, M.; Gordon, B.; Weiss, A. J.; Guzikowski, A. P. *J. Organomet. Chem.* **1978**, *51*, 77.

(19) Lee, J. F.; Lee, M. D.; Tseng, P. K. *Chemistry* **1987**, *45*, 50.

Table 4. Experimental and Crystal Data for the X-ray Structures

	14	**17**
formula	$C_{32}H_{34}Fe_2I_3$	$C_{32}H_{34}Fe_2$
M_r	911.03	530.31
cryst syst	orthorhombic	hexagonal
space group	*Pccn*	$P6_122$
a, Å	14.245(2)	7.631(2)
b, Å	15.112(2)	
c, Å	13.766(2)	68.711(8)
V, Å^3	2963.4(7)	3465.0(8)
Z	4	6
D_{calcd}, g cm^{-3}	2.042	1.525
μ, mm^{-1}	4.09	10.25
λ, Å	0.709 30	1.540 56
2θ limits, deg	44.8	119.8
max, min transm coeff	0.998, 0.750	0.9999, 0.2681
R_F	0.064	0.061
R_{wF}	0.070	0.069

after each run. These experiments were carried out with 1×10^{-3} M solutions of biferrocene in dry CH_2Cl_2/CH_3CN (1:1) containing 0.1 M of $(n\text{-}C_4H_9)_4NPF_6$ as supporting electrolyte. The potentials quoted in this work are relative to a Ag/AgCl electrode at 25 °C. Under these conditions, ferrocene shows a reversible one-electron oxidation wave ($E_{1/2} = 0.41$ V).

The single-crystal X-ray determinations of compounds **14** and **17** were carried out on an Enraf Nonius CAD4 diffractometer at 298 K. Absorption corrections were made with an empirical ψ rotation. The X-ray crystal data are summarized in Table 4. Listings of the complete tables of bond distances and angles, and thermal parameters of these compounds are given as Supporting Information.

Structure Determination of 17. An orange crystal (0.3 × 0.3 × 0.3 mm), which was grown by slow evaporation from a hexane solution, was used for data collection at 298 K. Cell dimensions were obtained from 20 reflections with 22.25° < 2θ < 32.63°. The $\theta-2\theta$ scan technique was used to record the intensities for all reflections for which 1° < 2θ < 119.8°. Of the 1201 unique reflections, there were 847 reflections with $F_o > 2.5\sigma(F_o^2)$, where $\sigma(F_o^2)$ were estimated from counting statistics. These data were used in the final refinement of the structural parameters.

A three-dimensional Patterson synthesis was used to determine the heavy-atom positions, which phased the data sufficiently well to permit location of the remaining non-hydrogen atoms from Fourier synthesis. All non-hydrogen atoms were refined anisotropically. During the final cycles of refinement fixed hydrogen contributions with C−H bond lengths fixed at 1.08 Å were applied. The final positional parameters for all atoms can be found in the Supporting Information, and the selected bond distances and angles are given in Table 1.

Structure Determination of 14. A black crystal (0.25 × 0.06 × 0.15 mm) was obtained when a layer of ether was allowed to slowly diffuse into a CH_2Cl_2 solution of **14**. Data were collected to a 2θ value of 44.8°. The cell dimensions were obtained from 25 reflections with 15° < 2θ < 30.32°. Of the 1932 unique reflections, there were 1033 reflections with $F_o^2 > 2.5\sigma(F_o^2)$. These data were used in the final refinement of the structural parameters.

Structure refinement was carried out in the same manner as described for **17**. The greatest residual electron density upon completion of refinement was in the vicinity of the iodide atoms. Selected bond distances and angles and atomic coordinates are given in Table 1 and the Supporting Information, respectively.

Acknowledgment. Our work was generously supported by the National Sun Yat-Sen University and the National Science Council (NSC85-2113-M-110-023) . We gratefully acknowledge this support.

Supporting Information Available: Complete tables of positional parameters, bond lengths and angles, and thermal parameters for **14** and **17** (10 pages). Ordering information is given on any current masthead page.

OM950968H